PAPER • **OPEN ACCESS**

Numerical studies of turbulent premixed flame interaction with repeated solid obstacles

To cite this article: M Elshimy *et al* 2020 *IOP Conf. Ser.: Mater. Sci. Eng.* **973** 012007

IOP Conf. Series: Materials Science and Engineering **973** (2020) 012007 doi:10.1088/1757-899X/973/1/012007

Numerical studies of turbulent premixed flame interaction with repeated solid obstacles

M Elshimy[1], S Ibrahim[1] and W Malalasekera[2]
[1]Department of Aeronautical and Automotive Engineering, Loughborough University, Loughborough, LE11 3TU, UK
[2]WolfsonSchool of Mechanical, Electrical and Manufacturing Engineering, Loughborough University, Loughborough, LE11 3TU, UK

m.a.a.a.elshimy@lboro.ac.uk

Abstract. This paper presents numerical simulations of hydrogen and propane turbulent premixed flames interaction with repeated solid obstructions. The laboratory-scale combustion chamber used in this study is equipped with three solid baffles which promote the generation of turbulence and a square obstacle located downstream from the ignition source. The test cases considered have two different area blockage ratios (ABR) of 24% and 50%, respectively. The large eddy simulation (LES) turbulence modelling technique is used. The numerical simulations are carried out using an in-house computational fluid dynamics (CFD) model. Two different flow configurations are examined, both using three consecutive baffles to identify the subsequent effects and the sensitivity of each fuel to increasing the ABR. These effects are studied using the nature of the flame-obstacles interaction, generated combustion overpressure and resultant flame speed. The modelling capability is confirmed by validating the numerical results against published experimental data. Conclusions are drawn that increasing the ABR increases the combustion overpressure, rate of pressure rise and flame speed. It is also concluded that the larger obstacle has a significant effect on the propagating flame structure and that hydrogen flames are more sensitive to an increased ABR and produce a significantly higher peak overpressure.

1. Introduction

The increasing scarcity of fossil fuels combined with a negative environmental impact has forced the search for an alternative fuel as a source of energy. Hydrogen (H_2) has been identified as a potential replacement for hydrocarbons due to its high energy density. Further, the use of hydrocarbons such as LPG (C_3H_8) or CNG (CH_4) as a fuel produces harmful greenhouse gases, unlike hydrogen. This presents a significant opportunity; however, research needs to be carried out to investigate the safety related factors in the production, storage and transport of the fuel [1]. Due to hydrogen's low ignition energy and wide flammability range it can pose a significant safety risk in an event where accidental ignition occurs [2]. The peak combustion overpressure is one of the main concerns in the event of an explosion and previous experiments have found that when compared to alternative hydrocarbons, hydrogen burns at much higher velocities and produces significantly higher peak combustion overpressures [3], [4].

The numerical results are validated against experimental data published by The University of Sydney, Australia [5]. Experiments concluded that by increasing the ABR and reducing the separation distance between successive solid obstructions the peak combustion overpressure and flame speed are increased [5]. This is due to the obstructions increasing the level of turbulence in the chamber which promotes combustion [3], [5].

Computational Fluid Dynamics (CFD) has become increasingly accepted as a substitute to experiments, enabling the numerical modelling of tests which may potentially be dangerous in a safe manner [6]. Large eddy simulations (LES) is used by researchers to study turbulent premixed flames in various applications [7-10]. Direct numerical simulations (DNS) can produce results to a high degree of accuracy, however it typically requires a large computational expense to do so. Reynolds-Averaged Navier-Stokes (RANS) is usually more fitting for large-scale applications. For appropriate results to be produced using LES, a suitable sub-grid-scale (SGS) model needs to be implemented in order to produce accurate results over a range of flow length scales. The present work uses the LES technique with a dynamic flame density model (DFSD)[11] to study the flame structure as it interacts with baffles and a solid obstacle before it propagates through the vented chamber.

Previous research has used the DFSD model to make accurate predictions for turbulent premixed flames propagating through baffles and past a solid obstacle [8], [12]. This research is further developed by investigating turbulent premixed flames for a stoichiometric propane-air mixture and alean hydrogen-air mixture (Φ=0.7). A comparison is made between the mixture interaction with three consecutive baffles and a solid obstruction with an area blockage ratio (ABR) of 24% and 50%.

2. Experimental Setup

The numerical results are validated using experimental data obtained from a lab-scale chamber constructed at The University of Sydney [3-5]. The combustion chamber measures 50 x 50 x 250 mm for a total volume of 0.625 liters. The chamber can be equipped with up to three removable baffle and

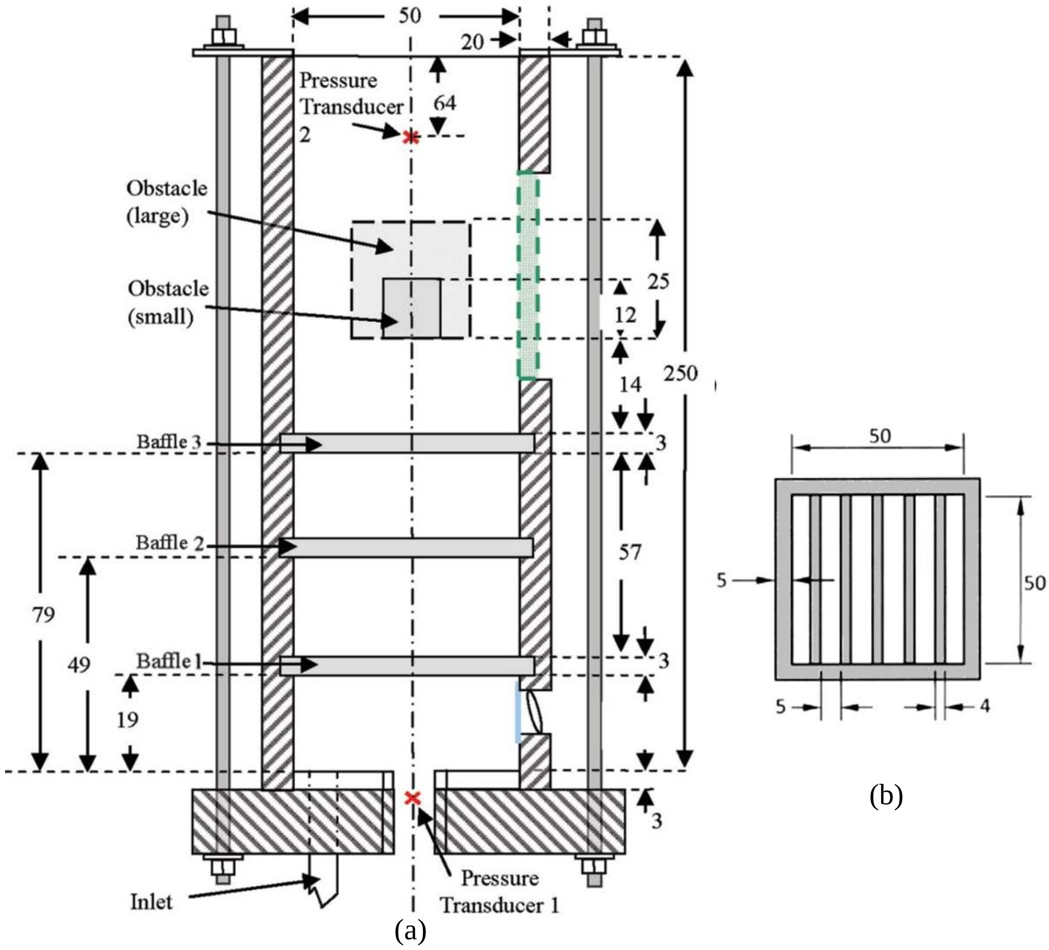

Figure 1. Chamber schematic (a) and removable baffle (b) (all dimensions in mm, not to scale).

a single solid obstacle as shown in figure 1. The solid obstruction is placed 96 mm from the base of the chamber with the option to use a small cubic obstacle with a side length of 12 mm and an ABR of 24% or a large cubic obstacle with a side length of 25 mm and an ABR of 50%. The baffles are located at 19 mm, 49 mm and 79 mm from the chamber base. Each baffle is made of five 4 mm wide and 3 mm thick strips evenly separated by 5 mm gaps. Each of the baffles provides an ABR of 40%.

The fuel-air mixture is introduced into the chamber using a non-return valve at atmospheric pressure and is allowed to settle before ignition occurs. Ignition is provided using an Nd:YA laser which produces an infrared output 2 mm above the base of the chamber, this identifies the start of the experiment. One second before ignition the vent at the top of the chamber is opened and remains open for the length of combustion. Experimental images are obtained using high-speed laser-induced fluoresce from OH at a rate of 5 kHz. Two Keller type PR21-SR piezo-electric pressure transducers attain pressure readings at a rate of 25kHz, with one transducer located in the base of the chamber and another in the wall of the chamber located 64 mm from the top vent.

Two different configurations are going to be studied utilizing three baffles and a small or large obstacle as shown in figure 2. Configuration BBBS uses baffles 1, 2 and 3 with the small square obstacle whereas configuration BBBL uses the three baffles combined with a large square obstacle.

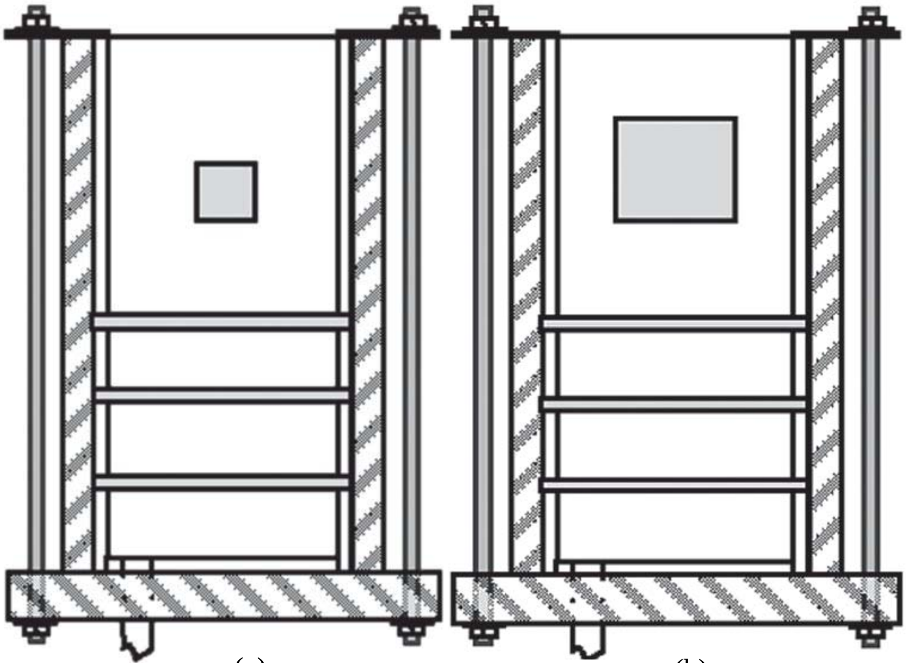

(a) (b)

Figure 2. Configuration BBBS with the small obstacle (a) and configuration BBBL with the large obstacle (b).

3. Numerical Setup

Numerical results are obtained using an in-house code known as PUFFIN developed by Kirkpatrick et al. The complete computational domain measures 325 x 325 x500 mm whereas the chamber measures 50 x 50 x 250 mm. The domain uses non-reflecting boundaries to avoid any influence of reflected pressure waves from the extended domain. The computational grid has a total of 2.7 million cells with 90 cells in the x and y directions and 336 cells in the z direction. This grid refinement has been used in previous research and is kept consistent for simulations using the small and large obstacle for both fuels [13]. Grid refinement varies in the z direction with areas of increased refinement where the flame interacts with and propagates past the baffles and the solid obstacle providing a more representative modeling of the flame propagation. The lean hydrogen-air mixture has a laminar burning velocity of 1.25 m/s and a laminar flame thickness of 0.12 mm. The propane-air mixture is composed of 95%

C_3H_8, 4% C_4H_{10} and 1% of other hydrocarbons by volume and has a laminar burning velocity of 0.39 m/s and a laminar flame thickness of 0.37 mm.

The laminar flamelet approach is used to model the mean reaction rate ($\bar{\dot{\omega}}$) using the equation:

$$\bar{\dot{\omega}} = \rho_u u_L \Sigma \quad (1)$$

Where ρ_u is the unburned mixture density, u_L is the laminar burning velocity and Σ is the Flame Surface Density (FSD).The FSD is dynamically modelled using a DFSD model. Further details on the DFSD model can be found elsewhere [11].

4. Results and Discussion

In this section numerical results are presented and discussed for a stoichiometric propane-air mixture (Φ=1.0) and a lean hydrogen air mixture (Φ=0.7). Numerical flame images are compared to LIF-OH images from experiments. Comparisons will be made between numerical results and experimental data for the overpressure-time histories, peak overpressure magnitude timing and magnitude as well as the maximum rate of pressure rise. The data presented in this paper is an average value obtained from 50 experiments [5]. Flame speed-time traces will also be presented and discussed.

4.1. Flame Images

The images shown below convey the flame obstacle interaction as the flame propagates through the baffles and past the larger solid obstacle. Experimental images shown in figure 3 for the propane-air mixture convey the flame as it jets through the final baffle and begins to interact with the large solid obstacle. The large flow generated wake behind the obstacle burns gradually as also shown in the numerical images in figure 4 as the flame continues to propagate through the chamber. Experimental images are not available for the hydrogen-air mixture due to experimental limitations, however numerical images are shown in figure 5. Research investigating these experiments concluded that further advanced equipment would be required to capture hydrogen combustion when using a large obstacle due to the extreme flame speeds [5]. Note the difference in times after ignition between figure 3 and figure 5 due to the hydrogen-air mixture reactivity.

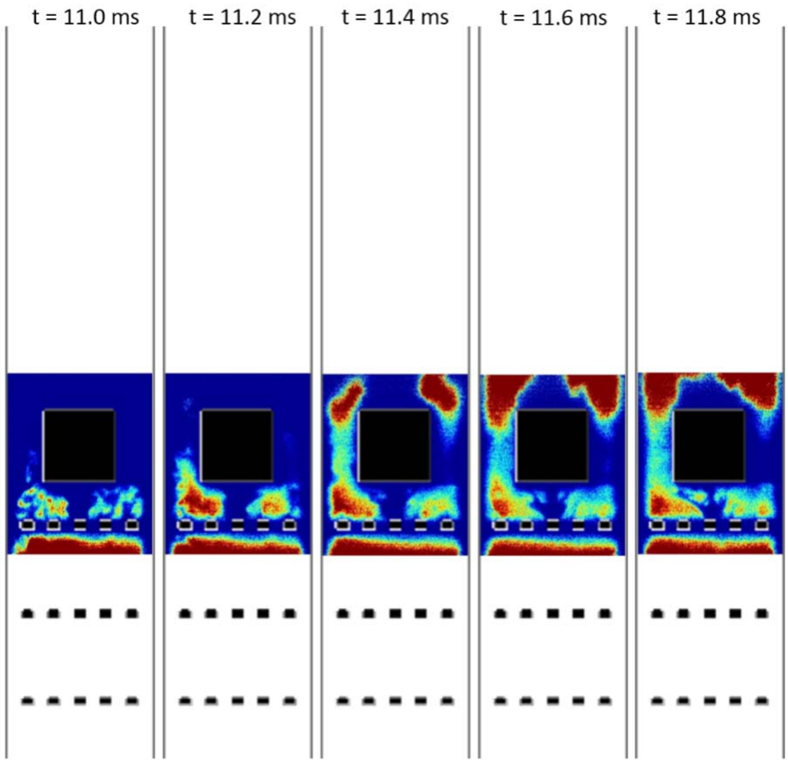

Figure 3. High Speed LIF-OH images of propane-air flame structure at different times after ignition.

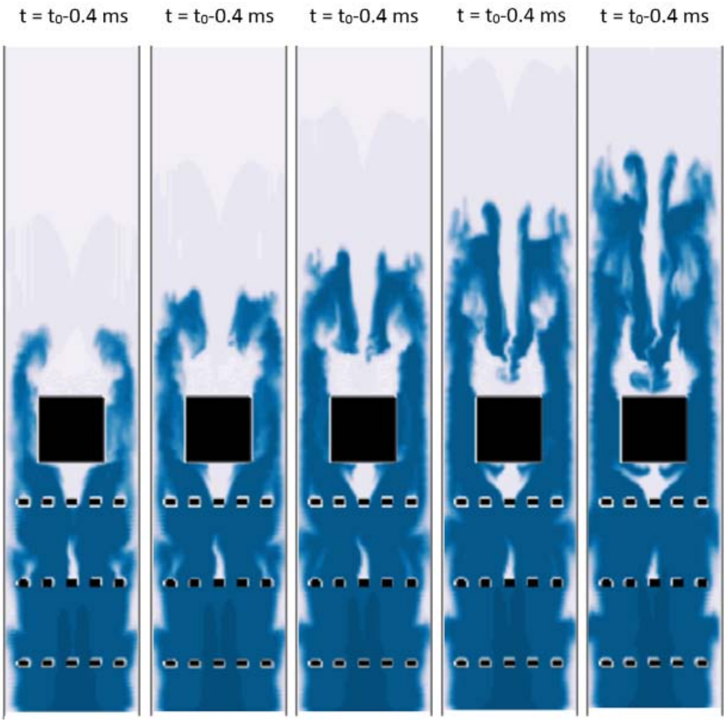

Figure 4. Numerical results showing Iso-lines of the reaction progress variable on the chamber midplane for propane-air flames.

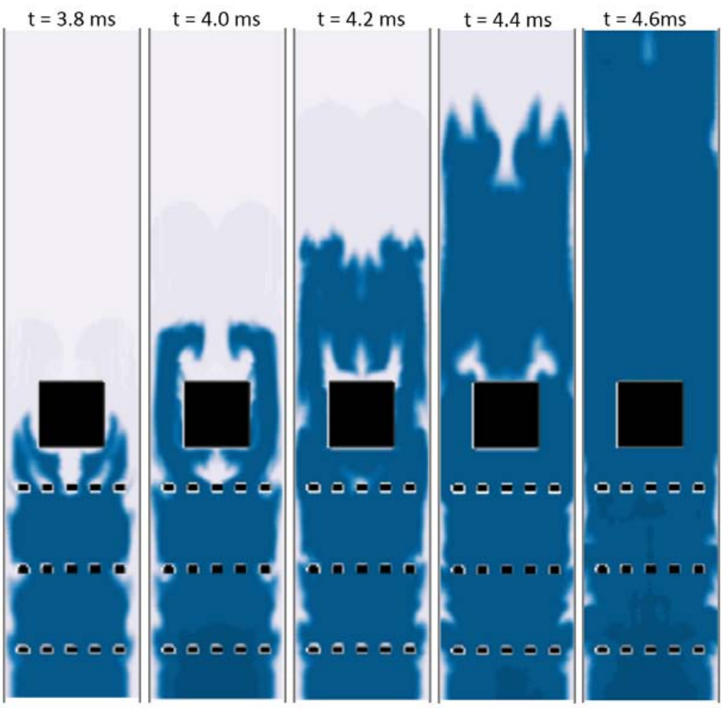

Figure 5. Numerical results showing Iso-lines of the reaction progress variable on the chamber midplane for hydrogen-air flames.

4.2. Overpressure Results

4.2.1. Peak Overpressure Timing. The time at which the maximum overpressure occurs is typically while the flame is propagating past the solid obstacle. This is due to the narrow passages on the sides of the obstacle followed by the flow generated wake behind the obstacle which provides a contribution to the overpressure magnitude when it is consumed. Tables 1 and 2 list the timing for the mixtures to reach the peak overpressure magnitude for the small and large obstacle. The lean hydrogen-air flames produce peak overpressure magnitude in less than half the time due to the mixture reactivity when compared to the stoichiometric propane-air flames.

IOP Conf. Series: Materials Science and Engineering **973** (2020) 012007 doi:10.1088/1757-899X/973/1/012007

Table 1. Comparison of the time peak overpressure magnitude occurs for hydrogen (Φ=0.7) and propane (Φ=1.0) using configuration BBBS.

	Hydrogen (ms)	Propane (ms)
Experimental Result	4.32	10.72
LES Result	4.15	10.52

Table 2. Comparison of the time peak overpressure magnitude occurs for hydrogen (Φ=0.7) and propane (Φ=1.0) using configuration BBBL.

	Hydrogen (ms)	Propane (ms)
Experimental Result	4.28	10.00
LES Result	4.44	10.37

4.2.2. Maximum Rate of Pressure Rise. The maximum rate of pressure rise will vary depending on the separation distance between obstructions, the fuel-air mixture strength and the ABR. Tables 3 and 4 below detail the maximum rate of pressure rise for the mixtures using the small and large solid obstacle. The maximum rate of pressure rise increases for both fuels with an increased ABR from 24% to 50%. Note that the lean hydrogen-air mixture has pressure that increases at a significantly higher rate when compared to the stoichiometric propane-air mixture.

Table 3. Comparison of the maximum rate of pressure rise for hydrogen (Φ=0.7) and propane (Φ=1.0) using configuration BBBS.

	Hydrogen (MPa/s)	Propane (MPa/s)
Experimental Result	320.51	8.53
LES Result	300.46	8.06

Table 4. Comparison of the maximum rate of pressure rise for hydrogen (Φ=0.7) and propane (Φ=1.0) using configuration BBBL.

	Hydrogen (MPa/s)	Propane (MPa/s)
Experimental Result	337.15	10.30
LES Result	349.56	13.85

4.2.3. Overpressure-time Traces. The pressure time histories presented convey various key events in the combustion process including the initial rise of pressure, the peak overpressure and the time at which the flame departs the chamber. When comparing figures 6 (a) and 7 (a) to figures 6 (b) and 7 (b) the hydrogen-air mixture produces a significantly higher magnitude of peak overpressure in a much shorter duration of time. Comparing figure 6 to figure 7 also conveys that increasing the ABR increases the peak overpressure magnitude for both fuels. The stoichiometric propane-air mixture produces a peak overpressure of 99.46 mbar using the smaller ABR which increases to 106.67 mbar. The lean hydrogen-air mixture is more sensitive to the increased ABR as it produces a peak magnitude of overpressure of 789.75 mbar which increases to 931.15 mbar using the larger ABR. The peak overpressure for the hydrogen-air mixture is almost ten-fold the peak propane-air mixture overpressure using an obstacle with an ABR of 50%.

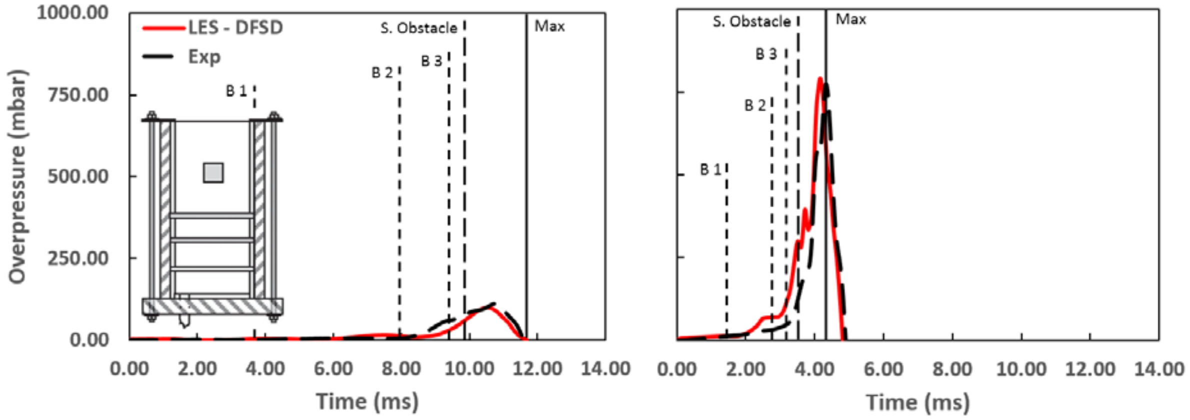

(a) (b)

Figure 6. Overpressure-time traces for propane-air at Φ=1.0 (a) hydrogen-air at Φ=0.7 (b) using configuration BBBS.

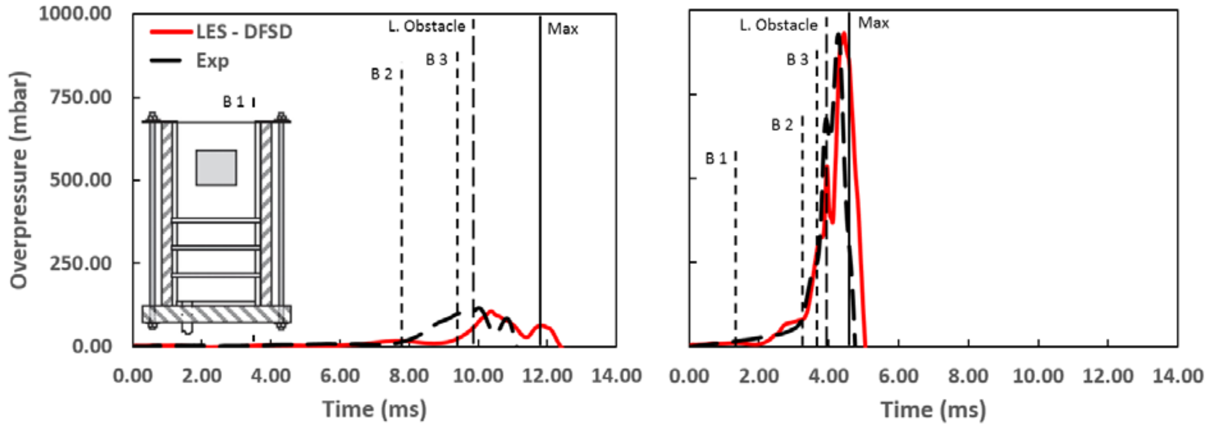

(a) (b)

Figure 7. Overpressure-time traces for propane-air at Φ=1.0 (a) hydrogen-air at Φ=0.7 (b) using configuration BBBL.

4.3. Flame Speed-Time Traces

Given the nature of the overpressure and rate of pressure rise results detailed it is expected that the combustion of the hydrogen-air mixture achieves significantly higher flame speeds in a shorter time period for both area blockage ratios when compared to the propane-air mixture.

figure 8 (a) clearly shows the increased speed with an increased ABR for the propane-air mixture. In figure 8 (b) this impact is less apparent for earlier phases of combustion, however the results presented convey that the increased ABR eventually increases the maximum flame speed as shown. Note that in figure 8 (b) the experimental speed-time data is not available for the configuration with the larger ABR due to the experimental limitations mentioned earlier.

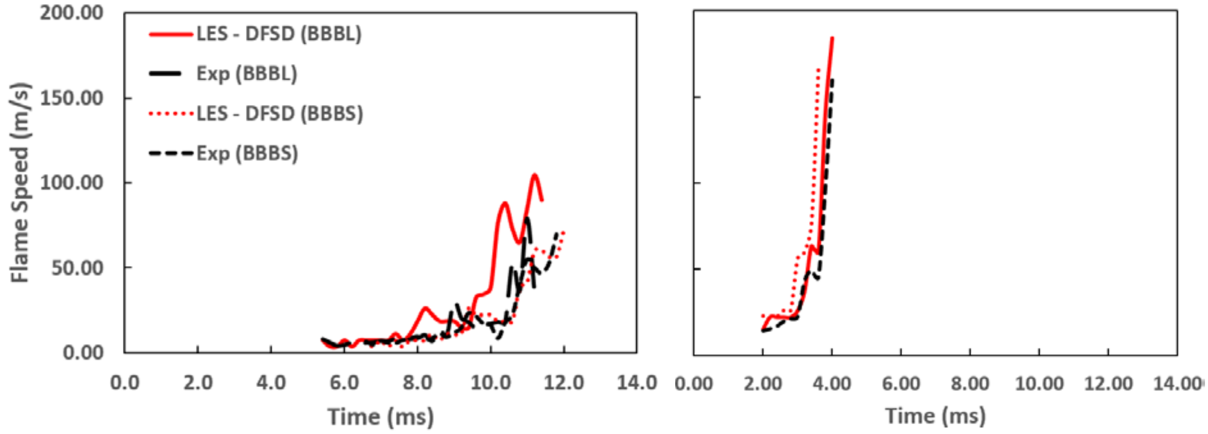

(a) (b)

Figure 8. Speed-time traces for propane-air at Φ=1.0 (a) hydrogen-air at Φ=0.7 (b).

5. Conclusions

This paper compares between numerical results obtained for the deflagration of hydrogen and propane flames using an ABR of 24% and 50%. The numerical results are validated against published experimental data and the following conclusions are drawn:

- Increasing the ABR increases the generated peak combustion overpressure and the maximum rate of pressure rise for both fuel-air mixtures.
- The combustion of hydrogen flames produces a significantly higher combustion overpressure at much higher flame speeds.
- Hydrogen flame deflagration takes place in a reduced amount of time due to the high mixture reactivity even at leaner mixture strength.
- Numerical calculations for the overpressure and flame speed produce good agreement for both fuel-air mixtures when compared with experimental data for both area blockage ratios.

References

[1] Marban, G and Valdes-Solis T 2007 Towards the hydrogen economy? *Int. J. Hydrogen Energy* **32** pp 1625-1637
[2] Bjerketvedt D, Roar Bakke J and Wingerden K V 1997 Gas explosion handbook *J. of Hazardous Materials* **52** pp 1-150
[3] Masri A R, AlHarbi A, Meares S and Ibrahim S S 2012 A comparative study of turbulent premixed flames propagating past repeated obstacles *I&EC research* **51**pp 7690-703
[4] AlHarbi A, Masri A R and Ibrahim S S 2014 Turbulent premixed flames of CNG, LPG and H_2 propagating past repeated obstacles *ETF science* **56**pp 2-8
[5] AlHarbi A 2013 Turbulent premixed flames propagating past repeated obstacles Ph.D. Thesis *The University of Sydney*
[6] Versteeg H K and Malalasekea W 2007 *An Introduction to Computational Fluid Dynamics – the Finite Volume Method* Pearson 2nd edition pp 40-113
[7] Pitsch H 2006 Large-eddy simulation of turbulent combustion *Annu. Rev. Fluid Mech.* **38** pp 453-482
[8] Masri A R, Ibrahim S S and Cadwallader B J 2006 Measurements and large eddy simulation of propagating premixed flames *Exp. Threm. Fluid Sci.* **30** pp 687-702
[9] Knikker R, Veyante D and Meneveau C 2004 A dynamic flame surface density model for large

eddy simulation of turbulent premixed combustion *Phys. Fluids* **16** pp L91-L94

[10] Charlette F, Meneveau C and Veyante D 2002 A power-law flame wrinkling model for LES of premixed turbulent combustion part II: dynamic formulation *Combust. Flame* **131** pp 181-197

[11] Gubba S R, Ibrahim S S, Malalasekera W and Masri A R 2007 Les modelling of propagating turbulent premixed flames using a dynamic flame surface density model *2nd ECCOMAS Thematic Conf. on Comp. Comb.* (Amsterdam: Delft)

[12] Ruipengyu Li, Malalasekera W and Ibrahim S 2018 Numerical study of vented hydrogen explosions in a small scale obstructed chamber *Int. J. Hydrogen Energy* **43** pp 16667-16683

[13] Gubba S R, Ibrahim S S, Malalasekera W and Mari A R 2011 Measurements and LES calculations of turbulent premixed flame propagation past repeated obstacles *Combust. Flame* **158** 12 pp 2465-2481